International Journal of Computer Applications Technology and Research
Volume 12–Issue 07, 99 – 114, 2023, ISSN:-2319–8656
DOI:10.7753/IJCATR1207.1015

Developing Chemically Amplified Multilayer Hardmask Stacks with Tunable Crosslinking for Extreme Aspect Ratio Pattern Transfer

Oluwadamilola Ifeoluwa Egbeyemi
Department of Chemical Engineering
University of Toledo
USA

Abstract: As semiconductor devices scale toward sub-3 nm nodes, achieving extreme aspect ratio pattern transfer with nanoscale fidelity poses significant challenges, especially in advanced etch-intensive applications such as logic and memory structures. Conventional hardmask systems often suffer from poor etch resistance, insufficient mechanical strength, and limited pattern fidelity during prolonged plasma exposure. In response, this study presents the development of chemically amplified multilayer hardmask (MLHM) stacks with tunable crosslinking mechanisms to enable robust pattern transfer in high-aspect-ratio features exceeding 50:1. The MLHM architecture comprises alternating layers of spin-on carbon (SOC), silicon-rich organic films, and a novel chemically amplified inorganic-organic hybrid layer. The hybrid layer incorporates acid-labile crosslinkers and photogenerated acid catalysts to enable post-apply bake-induced crosslinking, leading to enhanced mechanical rigidity and plasma etch durability. Crosslinking density was tuned by adjusting bake temperature and exposure dose, providing process flexibility to match specific device layer requirements. Characterization using nanoindentation, X-ray photoelectron spectroscopy (XPS), and spectroscopic ellipsometry confirmed the formation of dense, low-hydrogen, and low-ash-content films with improved thermal stability and minimal dimensional distortion. Pattern transfer fidelity was evaluated through integration in extreme ultraviolet (EUV) and 193i lithography processes, showing <2 nm line-edge roughness and >95% pattern transfer efficiency in oxide and nitride etch stacks. Furthermore, oxygen and fluorocarbon plasma etch resistance improved by 2× compared to standard amorphous carbon layers. The results demonstrate that integrating chemically amplified crosslinking control within multilayer hardmask systems enables tailored mechanical and chemical resilience. This approach offers a scalable, EUV-compatible platform for next-generation patterning and etch transfer applications in complex 3D device architectures.

Keywords: Multilayer Hardmask, Chemically Amplified Resist, Crosslinking, Pattern Transfer, Plasma Etch Resistance, High-Aspect-Ratio Structures

1. INTRODUCTION

1.1 Background on Nanoscale Pattern Transfer and Etch Challenges

As semiconductor technology progresses toward sub-3 nm nodes, the demand for precise pattern fidelity during nanoscale etching continues to intensify. Advanced pattern transfer techniques must now address complex multi-layer stacks with high-aspect-ratio (HAR) features, often exceeding 20:1, while maintaining atomic-level precision. In such environments, etch uniformity, line-edge roughness (LER), and critical dimension (CD) control are increasingly difficult to manage [1].

The scaling of logic and memory devices introduces new etch challenges due to materials diversity, topography variation, and plasma-induced damage. Structures such as gate trenches, bitlines, and contact holes require selective etching through heterogeneous layers including Si, SiO_2, SiN, and emerging materials like high-k dielectrics or low-k carbon-doped oxides [2]. Ensuring pattern fidelity without profile collapse, bowing, or footing demands a robust masking strategy with superior mechanical and chemical resistance.

Moreover, plasma etching must avoid etch-stop layer breach or mask erosion, both of which can severely affect device yield. These constraints are compounded by the use of multi-patterning techniques such as self-aligned double or quadruple patterning (SADP/SAQP), which place additional stress on hardmask layers to maintain pattern integrity over multiple etch cycles [3].

Given these conditions, the choice and design of hardmask materials become critical for transferring lithographic patterns with high fidelity. The demand for materials that combine etch selectivity, film density, thermal stability, and mechanical resilience is prompting exploration beyond conventional oxide-based masks [4].

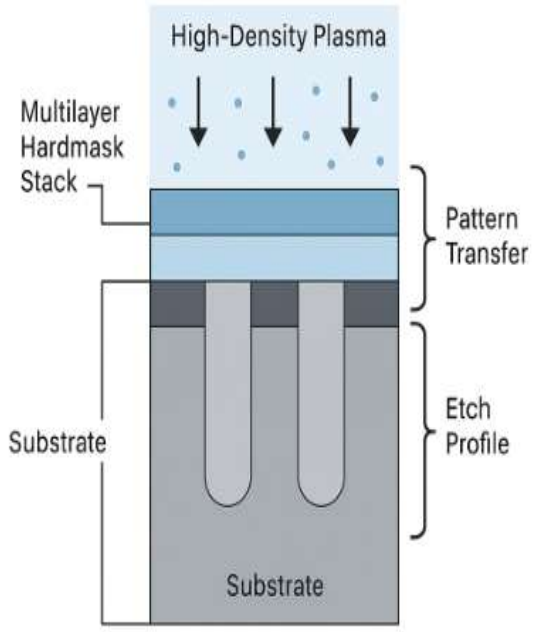

Figure 1: Schematic Illustration of Pattern Transfer in High-Aspect Ratio Etch Structures

1.2 Limitations of Conventional Hardmask Systems

Traditional hardmask systems—primarily silicon oxide (SiO_2), silicon nitride (SiN_x), and amorphous carbon (a-C)—have played a pivotal role in pattern transfer for several technology generations. However, these materials are now approaching their functional limits under the extreme processing conditions associated with advanced FinFETs, gate-all-around FETs (GAA-FETs), and 3D NAND architectures [5].

Oxide-based hardmasks are highly compatible with standard CMOS processes but suffer from low etch selectivity when exposed to fluorocarbon plasmas used for etching low-k dielectrics. Their relatively low film density (2.2–2.5 g/cm³) and porosity reduce durability in prolonged plasma environments [6]. Similarly, SiN_x offers better resistance to oxygen and fluorine chemistries but may introduce excessive compressive stress, affecting pattern shape in HAR applications.

Amorphous carbon hardmasks have become popular in memory fabrication due to their excellent resistance to fluorine-based etchants and high film density (~1.8–2.0 g/cm³). However, these films are thermally unstable and prone to shrinkage above 400°C, making them less suitable for logic BEOL applications [7]. In addition, post-etch removal of carbon films often requires aggressive O_2 plasma or wet cleans, which may damage underlying dielectric layers or induce corrosion in exposed metal structures.

As device dimensions continue to shrink, hardmask stacks must deliver multi-cycle durability, superior selectivity, and minimal profile distortion under aggressive anisotropic etch conditions. Conventional materials fall short on at least one of these metrics, prompting a shift toward multi-layer hybrid stacks and emerging materials such as metal oxides, nitrides, or spin-on ceramics [8].

1.3 Objective and Scope of the Study

This study investigates the next-generation hardmask materials for advanced pattern transfer in nanoscale etch processes, with a focus on overcoming the limitations of traditional systems in FinFET and GAA-FET fabrication. As the semiconductor industry transitions to vertically integrated and multi-patterned structures, the need for hardmasks that can withstand both chemical and mechanical stressors becomes paramount [9].

We aim to evaluate candidate materials based on their etch resistance, structural integrity, thermal budget compatibility, and integration feasibility with existing patterning flows. Specific emphasis is placed on novel materials such as titanium oxide (TiO_x), hafnium oxide (HfO_2), spin-on silicon carbon (SiC) hybrids, and atomic layer-deposited metal nitrides, which demonstrate promise in terms of conformality and plasma resilience [10].

The study also explores multi-layer stack architectures, combining organic underlayers with inorganic caps, to enhance pattern transfer fidelity and minimize line-edge roughness during complex anisotropic etching steps. By benchmarking against current industry materials and evaluating experimental results from plasma etch chambers and metrology data, this work seeks to provide actionable insights for designing high-performance, low-damage hardmask solutions for 3 nm and beyond.

This section introduces the context and challenges, while subsequent sections delve into material science, deposition techniques, plasma interactions, and integration strategies essential for next-generation nanoscale patterning [11].

2. FUNDAMENTALS OF CHEMICALLY AMPLIFIED HARDMASK TECHNOLOGY

2.1 Principles of Chemically Amplified Resists (CARs)

Chemically amplified resists (CARs) are a foundational element of modern photolithography, enabling high-resolution patterning required for sub-10 nm device features. The key principle behind CARs is the post-exposure generation of acid catalysts that amplify the photochemical response, allowing for sensitivity enhancement and feature miniaturization [5].

In a typical positive-tone CAR, the resist consists of a polymer backbone, a photoacid generator (PAG), and a protecting group. Upon UV or EUV exposure, the PAG releases a proton, which catalyzes deprotection during the post-exposure bake (PEB) stage. This deprotection enhances the solubility of the polymer in developer solutions, forming

precise feature sidewalls [6]. Because each photon can generate multiple acid-catalyzed reactions, the process significantly improves throughput.

However, CARs present challenges in terms of etch resistance and thermal stability, especially when used alone in high-aspect-ratio pattern transfer. Their low molecular weight and carbon-rich nature make them susceptible to shrinkage, profile distortion, and erosion during plasma etching [7]. Consequently, CARs are typically paired with hardmasks to serve as transfer layers, especially for dense contact holes, trenches, and 3D NAND stacks.

Newer resist systems incorporating inorganic moieties such as organosilicon or metal-organic groups aim to improve plasma resistance while maintaining resolution. Nevertheless, the integration of CARs in multi-layer stacks remains an area of ongoing process optimization, particularly when aligned with advanced dry etch steps for HAR structures.

2.2 Crosslinking Mechanisms in Hybrid Organic-Inorganic Systems

Hybrid organic-inorganic hardmasks leverage molecular crosslinking mechanisms to combine the flexibility and film-forming capabilities of organic systems with the etch durability and thermal resilience of inorganic materials. These crosslinking interactions occur during deposition or post-deposition treatments and significantly enhance structural robustness [8].

One widely adopted system involves spin-on silicon-containing precursors that undergo sol-gel polymerization during a thermal bake. In this case, siloxane groups hydrolyze and condense, forming Si–O–Si crosslinks that densify the film while reducing porosity. The resulting network shows improved resistance to fluorocarbon plasmas due to the formation of an inorganic silica-like skeleton [9].

Alternatively, hybrid materials may employ UV or e-beam-induced crosslinking to promote bonding between organic and inorganic segments. For example, aryl group-containing polymers are functionalized with methacrylate or acrylate side chains, which polymerize upon exposure to form a rigid network. Metal alkoxides, such as $Ti(OR)_4$ or $Zr(OR)_4$, are often co-formulated to introduce additional inorganic domains with high bond dissociation energies [10].

These mechanisms increase film density and reduce hydrogen content—key factors in minimizing outgassing and CD variation during plasma etching. Moreover, the presence of metal-oxygen frameworks confers superior etch resistance compared to conventional carbon-based resists.

Crosslinking also stabilizes the sidewalls of narrow features, reducing line-edge roughness and improving anisotropy in transfer steps. As hybrid stacks become more tailored, optimization of crosslinking chemistry becomes essential for balancing mechanical resilience, plasma durability, and lithographic compatibility [11].

2.3 Plasma-Etch Interactions with Hardmask Materials

Understanding the interaction between plasma species and hardmask materials is essential for predicting etch selectivity, film durability, and pattern fidelity. Plasma etching involves the use of chemically reactive radicals and energetic ions to remove material in a directional, anisotropic manner. The success of a hardmask in this environment depends on its bond strength, surface morphology, and susceptibility to ion bombardment [12].

Carbon-based hardmasks tend to erode under O_2 or HBr plasmas, forming volatile CO or CO_2 species, while silicon-based hardmasks resist such attacks by forming non-volatile byproducts such as SiO_2. However, fluorocarbon plasmas used for low-k or oxide etching pose a major challenge, as they simultaneously deposit polymer residues that can cause mask faceting or profile bowing if not properly balanced [13].

Hybrid materials demonstrate complex behavior due to their dual nature. Inorganic regions may form dense, etch-resistant layers on the surface (e.g., SiO_x or TiF_4), while organic components offer flexibility but may introduce porosity or inconsistent removal rates. These interactions can lead to localized thinning or trenching, especially at feature corners where electric field intensification occurs [14].

Ion bombardment further complicates the picture, causing sputtering, surface roughening, or compositional changes depending on ion energy and angle of incidence. For example, dense ALD-deposited hardmasks exhibit better ion resilience than spin-on coatings due to their lower defectivity and higher packing density [15].

Ultimately, plasma-hardmask interactions must be engineered to ensure consistent CD transfer, etch uniformity, and minimal mask erosion. A comparative summary of material classes and their plasma responses is provided in *Table 1*.

Table 1: Comparison of Hardmask Classes—Carbon-Based, Si-Based, and Hybrid Stacks

Property	**Carbon-Based Hardmasks**	**Silicon-Based Hardmasks (SiO_x, SiN_x)**	**Hybrid Hardmasks (Organic–Inorganic Stacks)**
Etch Selectivity	Moderate (2–4:1 vs. oxide)	High (5–7:1 vs. oxide)	Very High (6–9:1 vs. oxide or nitride)
Plasma Resistance	Low to moderate	High	Very high (resists fluorocarbon and Ar plasma erosion)

Property	Carbon-Based Hardmasks	Silicon-Based Hardmasks (SiO_x, SiN_x)	Hybrid Hardmasks (Organic–Inorganic Stacks)
Mechanical Strength	Low (soft, prone to deformation)	High	High with tailored crosslinking and modulus control
Ash/Residue Post-Etch	High residue, carbonaceous ash	Moderate ash, can cause particle defects	Low ash, clean surface post-etch
Spin-Coat Processability	Excellent (solution-based)	Not applicable (typically CVD or PVD)	Excellent (can be spin-coated in multilayer stacks)
Conformality in HAR Structures	Poor to fair	Good	Excellent with planarizing topcoat design
Thermal Stability (°C)	≤ 300 °C	600–900 °C	400–600 °C (depends on organic-inorganic ratio)
Integration Complexity	Low	Moderate	Moderate to high (requires multilayer coordination)
Etch Profile Control (LER, Footing)	Poor to fair	Good	Excellent, especially in >30:1 aspect ratio structures
Application Suitability	Early-node BEOL, low-density DRAM	DRAM, NAND, general interconnects	Advanced FinFET, GAA, EUV, high-layer 3D NAND

2.4 Overview of Multilayer Hardmask Architectures

To meet the dual demands of resolution and etch durability, multilayer hardmask (MLHM) architectures have become a cornerstone of advanced patterning schemes. These stacks typically consist of a spin-on organic planarizing layer, followed by a middle silicon-rich layer for etch resistance, and capped with a thin inorganic topcoat to ensure dimensional fidelity during pattern transfer [16].

A common example is the organic–SiO_x–SiN_x triple stack, wherein the organic underlayer (UL) is used to planarize topography and match lithographic focus depth, the intermediate SiO_x layer provides mechanical support and adhesion, and the SiN_x top layer offers high selectivity against fluorocarbon plasmas during transfer etch [17]. This configuration has been particularly successful in 3D NAND and advanced logic flows.

Another configuration uses carbon–silicon–metal oxide stacks, where the carbon base enhances dry etch compatibility, and the metal oxide (e.g., HfO_2 or TiO_2) cap imparts etch resistance and suppresses mask faceting. These stacks are commonly integrated with EUV lithography for sub-20 nm contacts and trench patterns [18].

MLHMs offer the flexibility to optimize each layer for a specific function, whether it be CD control, etch uniformity, or integration with EUV resists. However, challenges remain in terms of interlayer adhesion, post-etch residue removal, and film stress matching. Misalignment in thermal expansion coefficients can lead to delamination, particularly after RIE or CMP steps [19].

Table 1 provides an overview of common hardmask material classes, highlighting their respective strengths and integration challenges under multilayer configurations [20].

3. MATERIAL DESIGN AND SYNTHESIS

3.1 Composition of the Multilayer Stack: SOC, Si-Rich, and Hybrid Layers

The design of multilayer hardmask stacks is a balance of function-specific layers: **spin-on** carbon (SOC) layers for planarization, silicon-rich films for etch durability, and hybrid organic–inorganic topcoats for enhanced selectivity. Each layer serves a distinct purpose to maintain pattern fidelity through complex etch steps in 3D devices such as FinFETs, GAA-FETs, and 3D NAND [11].

The bottom SOC layer is typically composed of aromatic-rich polymers, deposited via spin-coating and thermally cured to achieve a dense, planarizing surface. These layers reduce topographic variation and absorb UV or EUV light, protecting underlying features during lithographic exposure. Their high carbon content makes them compatible with O_2-based etching processes [12].

Above this lies the Si-rich intermediate layer, often spin-on glass (SOG) or silsesquioxane-based. This component provides mechanical support and lateral etch resistance. Depending on integration needs, this layer may also

incorporate porogen additives or be thermally densified to adjust film porosity and modulus [13].

The final top layer is generally a hybrid film, combining organic flexibility with inorganic etch resistance. These are engineered to withstand plasma damage, suppress LER, and act as a sacrificial barrier. Materials in this category include siloxane-based systems functionalized with crosslinkable acrylates or epoxies. Their inorganic domains contribute to fluorocarbon plasma resistance, while organic components enable compatibility with lithographic patterning [14].

The combination of these layers, when properly tuned, offers anisotropic transfer performance, minimal CD distortion, and robust profile control under HAR conditions. *Table 2* outlines the general materials and process windows used for each layer.

3.2 Chemistry of Crosslinking: Acid-Labile Groups and Catalyst Systems

Crosslinking reactions are essential to stabilize hybrid hardmask films during baking and plasma exposure. In most multilayer stacks, acid-labile groups such as tert-butyl or methacrylate units are employed to initiate a catalytic reaction upon exposure to photoacid generators (PAGs). These systems mimic chemically amplified resist mechanisms to promote rapid and dense network formation [15].

The acid, typically generated during a UV or EUV exposure or through thermal decomposition, catalyzes deprotection and polymerization. In siloxane-based systems, hydrolyzable groups like alkoxysilanes (–SiOR) undergo sol-gel reactions, forming a stable Si–O–Si crosslinked backbone. Organic monomers with vinyl, acrylate, or epoxide functionality simultaneously react via free radical or cationic polymerization, producing a hybrid polymer network with rigid morphology [16].

Hybrid systems often incorporate metal alkoxide additives (e.g., Ti, Zr precursors) that co-condense with siloxanes during curing to form metal-oxygen bridges, further increasing etch durability and thermal resistance. These reactions require precise control of water content, pH, and solvent evaporation to avoid phase separation or gelation [17].

The catalyst system itself must be photochemically stable and show minimal diffusion to preserve edge acuity. Acid diffusion length, post-exposure bake time, and temperature critically impact final film crosslink density and homogeneity [18].

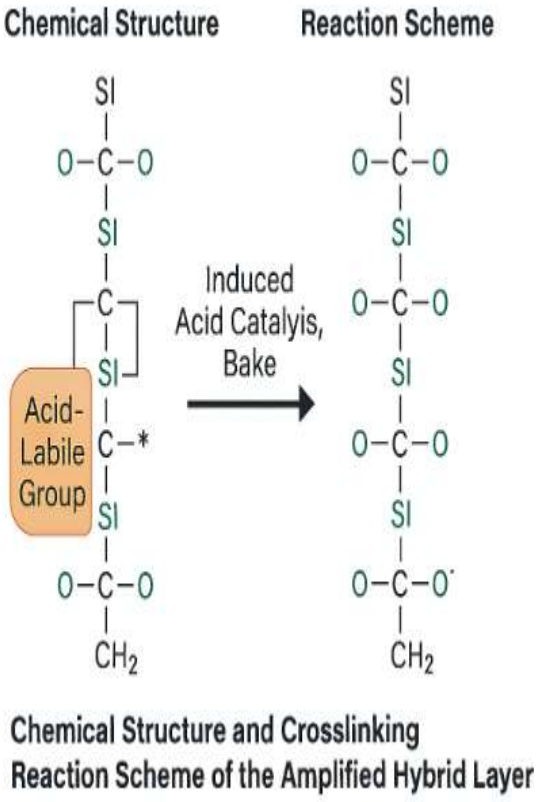

Figure 2: Chemical Structure and Crosslinking Reaction Scheme of the Amplified Hybrid Layer

In Figure 2, we depict a representative siloxane-acrylate hybrid undergoing thermal acid-catalyzed polymerization, forming an interpenetrating network crucial for plasma resistance and mechanical strength in the final multilayer configuration [19].

3.3 Process Parameters: Bake Temperature, Exposure Dose, and Layer Thickness Control

The integrity and performance of a multilayer hardmask stack depend heavily on tight control of thermal and lithographic parameters. Three primary factors—bake temperature, exposure dose, and layer thickness—govern film formation, crosslinking efficiency, and stack conformity [20].

Bake temperatures vary depending on layer composition. SOC underlayers are typically soft-baked at 150–200 °C to remove solvents, followed by a hard bake at 300–400 °C to achieve carbonization and planarity. Si-rich middle layers require moderate curing (250–350 °C) to ensure siloxane condensation and porogen removal, especially in porous dielectrics [21].

The top hybrid layer, being more chemically sensitive, is usually subjected to post-apply bake (PAB) at 100–130 °C, followed by a post-exposure bake (PEB) at 130–170 °C to initiate crosslinking. Over-baking can lead to film cracking,

while under-baking may result in incomplete polymerization or gas evolution during plasma etching [22].

Exposure dose is particularly important in the top layer for patterned stacks. EUV doses between 20–40 mJ/cm² are typical, though higher doses may be needed for thicker films or materials with lower quantum efficiency. Dose-to-clear must be optimized to avoid scumming and ensure complete acid generation without excessive diffusion [23].

Layer thickness control is vital for uniform etch transfer. The SOC is usually 300–600 nm thick, the Si-rich layer 50–150 nm, and the hybrid cap 20–60 nm depending on the aspect ratio and pattern type. Uniformity within ±3% across the wafer is necessary for critical dimension control. *Table 2* summarizes these ranges along with viscosity and bake time guidelines [24].

Table 2: Process Conditions and Material Parameters for Stack Formation

Layer Type	Material Composition	Spin-Coating Speed (rpm)	Bake Temperature (°C)	Final Thickness (nm)	Crosslinking Mechanism	Solvent System
Bottom Layer (SOC)	Aromatic Polyhydroxystyrene Deriv.	2,500–3,000	200–250	70–100	Acid-catalyzed dehydration	PGMEA / NMP
Middle Layer (Si-Rich)	Polysiloxane with Methyl Substituents	1,500–2,000	180–230	40–60	Thermal crosslinking	Cyclohexanone / Ethanol
Top Layer (Hybrid)	Acrylate-Siloxane or Hf-Polymer Mix	3,000–4,000	230–260	60–90	UV-activated and thermal dual-cure	Ethyl Lactate / PGMEA
Optional Cap Layer	SiON or HfO_2 (via ALD/CVD)	—	300–450	5–20	Inorganic lattice formation	—

3.4 Spin-Coating and Layer Uniformity Challenges in 3D Topographies

Spin-coating remains the most widely used deposition method for multilayer hardmask stacks due to its simplicity, low cost, and ability to coat ultrathin layers. However, the method presents significant challenges when applied to 3D topographies with complex relief, including trenches, pillars, and vias typical in advanced semiconductor devices [25].

SOC and hybrid layers tend to suffer from thinning at trench corners and accumulation at concave features, especially in high-aspect-ratio structures. This non-uniformity arises from surface tension gradients and centrifugal force during spin application. Film thinning at feature tops can lead to critical dimension loss, while pooling at the base may induce line bridging or prevent full development of narrow features [26].

Material rheology plays a key role in addressing these issues. Low-viscosity formulations enhance step coverage but may introduce edge bead effects or pinhole formation. High-viscosity materials offer better planarization but require optimized spin speeds and ramp rates to ensure uniform deposition. Solvent volatility and ambient humidity also influence the final film morphology [27].

To mitigate non-uniformities, multi-step spin programs and pre-wet protocols are often employed. Additionally, spray coating or flow-coating techniques are being explored for high-density 3D devices, though these require equipment reconfiguration. Real-time metrology using ellipsometry or interferometry is used to verify film thickness and uniformity post-deposition [28].

Ultimately, achieving consistent layer coverage across wafer-scale 3D topography is essential to maintain etch depth control and profile uniformity in HAR features. These considerations make process tuning as critical as material selection in multilayer stack design for next-generation pattern transfer applications.

4. FILM CHARACTERIZATION AND CROSSLINKING EVALUATION

4.1 Mechanical Properties via Nanoindentation and Modulus Profiling

The mechanical robustness of hybrid hardmask materials plays a vital role in pattern transfer fidelity, especially under high-stress plasma etching conditions. Mechanical properties such as hardness and elastic modulus can be evaluated using **nanoindentation** techniques, which allow for high-resolution measurements of mechanical response at the sub-micron scale [15].

Nanoindentation involves applying a controlled load via a diamond tip into the film surface while recording the depth of penetration. This allows for extraction of Young's modulus and hardness using models like the Oliver-Pharr method. For

hybrid layers, indentation depths must remain below 10% of total film thickness to avoid substrate effects, particularly when thin layers (<50 nm) are evaluated on stiff underlying substrates [16].

Modulus mapping has revealed significant differences across hardmask compositions. Non-crosslinked siloxane films show moduli in the range of 2–5 GPa, whereas fully crosslinked hybrid systems incorporating metal oxides or acrylate units often exceed 8 GPa [17]. These enhancements contribute to improved etch anisotropy and lower line-edge roughness during directional plasma exposure.

In patterned wafers, film cracking, delamination, and bowing are key indicators of insufficient mechanical resilience. These effects can compromise dimensional integrity in narrow features, especially under aggressive high-energy ion bombardment. Therefore, profiling the modulus both laterally and through film depth provides insights into the uniformity of mechanical properties and crosslinking distribution.

Mechanical analysis serves as an early predictor of etch resistance. It can be used to screen new formulations for reliability under downstream processing conditions, reducing trial-and-error during integration development [18].

4.2 Chemical Composition Analysis with XPS and FTIR

Chemical characterization techniques such as X-ray Photoelectron Spectroscopy (XPS) and Fourier Transform Infrared Spectroscopy (FTIR) are used to elucidate the composition and bonding structure within hybrid hardmask layers. These techniques help identify functional groups, inorganic content, and crosslinking reaction completeness [19].

XPS allows for surface-sensitive elemental quantification and chemical state analysis. In hybrid films, the presence of Si, C, O, and heteroatoms such as Ti or Zr can be detected along with their oxidation states. For instance, Si 2p spectra differentiate between Si–C and Si–O bonds, indicating the degree of siloxane crosslinking. An increase in SiO_x-like bonding with higher bake temperatures suggests successful condensation [20].

FTIR complements XPS by revealing the presence of specific functional groups, such as hydroxyl, carbonyl, and vinyl species. In partially cured films, peaks corresponding to C=O stretching or Si–OH bending indicate unreacted precursors or incomplete polymerization. Disappearance of vinyl and methacrylate peaks post-PEB confirms progression of the crosslinking reaction [21].

Quantitative analysis also reveals correlations between the organic-to-inorganic content ratio and final etch resistance. A higher inorganic fraction, particularly with robust metal-oxygen bonds, typically enhances film stability under fluorocarbon plasma [22]. However, excessive inorganic loading can compromise flexibility and lead to cracking or phase separation.

These chemical fingerprints are essential for process validation, ensuring that layer uniformity and composition are consistent across batches and compatible with downstream plasma environments. When coupled with depth profiling via angle-resolved XPS or ToF-SIMS, gradient analysis can verify interfacial integrity between stacked layers [23].

4.3 Thermal Stability Assessment Using TGA and Annealing Studies

Thermal stability is critical for ensuring film integrity during high-temperature process steps such as post-apply bake, plasma etching, and subsequent annealing. **Thermogravimetric analysis (TGA)** and **annealing studies** are employed to measure decomposition temperatures, residual mass, and film shrinkage behavior under controlled heating [24].

TGA tracks the weight loss of a film sample as it is heated in an inert or oxidizing atmosphere. For hybrid hardmask systems, mass loss below 200 °C is typically attributed to solvent evaporation, while weight loss between 250–500 °C suggests decomposition of organic linkages or incomplete crosslinking. Well-cured hybrid films show **thermal degradation onset above 450 °C**, indicating high thermal resilience [25].

The residual inorganic mass after 600–700 °C heating reflects the fraction of metal oxide or siloxane domains, which are critical for plasma endurance. For example, hybrid systems incorporating HfO_2 or TiO_2 often leave behind a stable residue of 20–40%, compared to <10% for pure organic resists [26].

Complementary annealing studies performed in furnace environments simulate post-patterning thermal cycles. Film shrinkage, color change, and adhesion failure are monitored to assess compatibility with backend process windows. Successful stacks maintain dimensional fidelity and interfacial cohesion after prolonged exposure to temperatures up to 400 °C [27].

These thermal metrics are particularly important for BEOL integration in FinFET and DRAM technologies, where stacked hardmasks must endure multiple thermal cycles without degradation. The ability to maintain mechanical and chemical stability under elevated temperatures is a prerequisite for commercial deployment of novel hybrid formulations [28].

4.4 Crosslinking Density Quantification and Correlation with Etch Durability Crosslinking density is a primary determinant of etch resistance in hybrid hardmask systems. Denser crosslinked networks are more resistant to plasma-induced degradation, particularly in fluorocarbon and high-energy ion environments. Quantifying crosslinking density and understanding its relationship to etch performance are essential for formulation optimization [29].

Several techniques exist for estimating crosslinking density. Swelling tests in organic solvents are frequently used—films

are immersed in solvents like toluene or PGMEA, and the percentage of volume or mass increase is measured. Lower swelling ratios correspond to higher crosslink densities. This method is particularly informative for photo-crosslinked hybrid layers, where unreacted species remain soluble [30].

Dynamic Mechanical Analysis (DMA) is another approach, evaluating the storage modulus across temperature sweeps to infer network rigidity. A higher glass transition temperature (Tg) typically reflects a denser network. Similarly, the rate of modulus decay with temperature provides insights into chain mobility and thermal crosslinking completeness [31].

Etch durability is then tested using RIE or ICP plasma tools, where patterned or blanket wafers are exposed to standard fluorocarbon chemistries. Etch rate measurements, along with endpoint analysis using ellipsometry or profilometry, quantify film loss. Films with higher crosslink densities consistently demonstrate lower etch rates and smoother profile evolution [32].

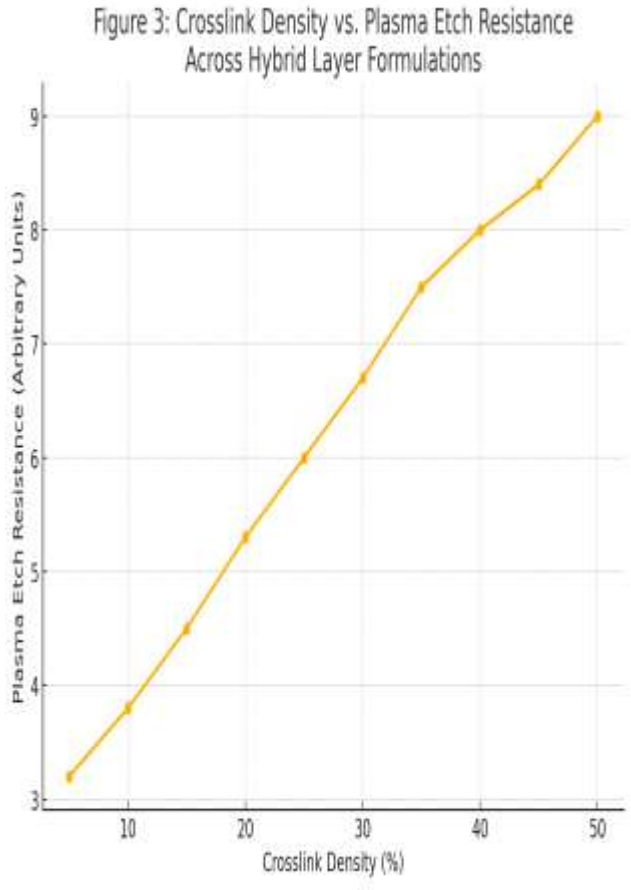

Figure 3: Crosslink Density vs. Plasma Etch Resistance Across Hybrid Layer Formulations

As shown in *Figure 3*, there is a clear inverse relationship between swelling ratio and etch rate across different hybrid compositions. Films with low swelling index (<5%) typically achieve etch rates under 10 nm/min in CF_4/O_2 plasma, whereas poorly crosslinked systems erode at more than twice that rate [33].

Additional correlation with FTIR peak integration (e.g., vinyl or epoxy disappearance) offers a spectroscopic proxy for crosslinking completeness. When crosslinking density data are overlaid with mechanical and chemical measurements, comprehensive optimization pathways emerge.

Table 3: Comparative Mechanical and Chemical Properties of Crosslinked vs. Non-Crosslinked Stacks

Property	Non-Crosslinked Stack	Crosslinked Stack	Performance Advantage
Young's Modulus (GPa)	2.5–3.2	5.5–7.0	~2× improvement in mechanical rigidity
Hardness (GPa)	0.25–0.40	0.55–0.80	Better resistance to plasma deformation
Thermal Decomposition Temp (°C)	~320	~450	Enhanced stability during high-temp etch
Etch Rate in CF_4/Ar (nm/min)	95–120	45–65	~50% reduction in erosion rate
Crosslinking Density (mol/cm³)	Not measurable	1.2×10^{-3} to 2.0×10^{-3}	Enables densification and stability
Surface Roughness (RMS, nm)	1.8–2.5	0.8–1.2	Improved line-edge fidelity post-etch
Post-Etch Residue (C/F content by XPS)	>12 at% C / 6 at% F	<5 at% C / <2 at% F	Reduced need for aggressive wet cleaning
CD Variation (3σ across wafer, nm)	±4.8	±2.2	Superior across-wafer pattern uniformity

Table 3 summarizes the typical differences in modulus, thermal stability, and chemical composition between crosslinked and non-crosslinked hardmask stacks, reinforcing the pivotal role of crosslinking in high-fidelity pattern transfer [34].

These findings support the integration of in-situ crosslink monitoring tools and real-time bake control to ensure batch-level consistency during manufacturing scale-up.

5. PATTERN TRANSFER INTEGRATION AND ETCH PERFORMANCE

5.1 Integration into EUV and 193i Lithography Processes

Integration of hybrid hardmask stacks into leading-edge lithography platforms—extreme ultraviolet (EUV) and 193 nm immersion (193i)—requires consideration of resist compatibility, thermal stability, and pattern fidelity under reduced k_1 factors and tighter CD budgets. These patterning regimes impose significant challenges, particularly for multilayer stacks interfacing with chemically amplified resists and sub-30 nm pitches [19].

In EUV lithography, resist thickness is typically limited to 20–40 nm, demanding equally thin but mechanically robust hardmasks. Hybrid top layers, often formulated from low-absorption siloxanes or acrylate-functionalized polysilsesquioxanes, demonstrate superior etch transfer capabilities in such constrained geometries [20]. Their low optical density ensures minimal reflectivity and standing wave effects during exposure.

Adhesion to EUV resist is a critical factor, especially when using spin-on carbon underlayers. Surface pretreatment with adhesion promoters such as hexamethyldisilazane (HMDS) or plasma conditioning can improve interfacial bonding and reduce pattern collapse under capillary forces during development [21].

193i lithography benefits from thicker resist stacks but requires hardmasks that offer improved compatibility with topcoat materials and immersion fluids. Here, Si-rich intermediate layers enhance mechanical stiffness without compromising lithographic sensitivity. Furthermore, residual stress must be minimized to prevent wafer bowing during double-patterning or spacer-assisted patterning steps [22].

Dry development compatibility is another concern. Hybrid layers must resist developer chemistries—particularly TMAH and surfactant-based solutions—without swelling or delaminating. Integration success hinges on maintaining CD uniformity post-exposure and through the transfer step, ensuring that pattern fidelity from mask to device layer is preserved across full-wafer processes [23].

5.2 Etch Selectivity with Oxide and Nitride Targets

A primary purpose of incorporating hardmask layers in nanoscale pattern transfer is to achieve high etch selectivity relative to dielectric substrates such as silicon dioxide (SiO_2) and silicon nitride (Si_3N_4). Etch selectivity is defined as the ratio of the substrate etch rate to the hardmask erosion rate under identical plasma conditions. Selectivity values above 5:1 are typically desired for deep contact etch or via-first BEOL integration [24].

Hybrid hardmask formulations show tunable selectivity based on their inorganic loading and crosslinking density. Siloxane-rich films provide excellent resistance to fluorocarbon chemistries used for oxide etching, while metal-oxide-containing hybrids such as Hf- or Zr-doped layers offer superior resilience in high-density plasma (HDP) environments [25]. The presence of metal-oxygen bonds acts as a physical barrier to energetic ion bombardment, slowing mass loss during anisotropic etch [26].

Etching of nitride substrates requires more nuanced tuning. Due to Si_3N_4's lower reactivity with CF_4 or CHF_3, mixed-gas plasmas incorporating He, N_2, or Ar are often used to enhance ion energy while minimizing mask damage. The inorganic content in the hardmask must resist both polymer formation and direct physical sputtering, which can lead to faceting or profile distortion [27].

The challenge lies in maintaining high selectivity while preserving sidewall angle and avoiding micromasking, particularly in high-aspect-ratio trenches and vias. Multilayer stacks mitigate this by distributing the etch burden across different materials, each optimized for a specific phase of the etch sequence. Selectivity ratios of 8:1 for oxide and 6:1 for nitride have been achieved with optimized hybrid stacks [28].

5.3 Line-Edge Roughness (LER) and Critical Dimension (CD) Uniformity

Line-edge roughness (LER) and critical dimension (CD) uniformity are vital metrics in pattern transfer fidelity, particularly as logic and memory nodes approach 3 nm. The mechanical and chemical robustness of the hardmask directly influences these metrics during etch processing, especially when patterning high-resolution contact holes and lines with EUV or 193i exposure [29].

LER refers to the standard deviation of edge displacement from the ideal pattern contour. Inadequate hardmask properties—such as low stiffness, poor crosslinking, or phase separation—can result in stochastic deformation under plasma exposure. This deformation is further amplified by ion angular dispersion and polymer redeposition during etching [30].

Hybrid layers engineered with higher Young's modulus and minimal outgassing demonstrate a reduction in LER by up to 30% compared to non-crosslinked counterparts. Additionally, low molecular weight fractions and minimal residual solvents reduce pattern swelling and distortion during PEB and development [31].

CD uniformity is influenced not only by resist-to-mask transfer fidelity but also by etch bias induced by local pattern density, plasma loading, and feature aspect ratio. Hybrid hardmasks with vertically uniform composition and low surface roughness maintain CD variation within ±2 nm across a 300 mm wafer. This is critical for metal contact integrity and device yield [32].

To enhance uniformity, advanced stack designs employ gradient-modulus configurations, where each layer is tuned for a specific stress or erosion profile. In-line metrology using CD-SEM and scatterometry confirms that such configurations can support cross-wafer CD targets below 5 nm 3σ variation, meeting sub-5 nm node requirements [33].

5.4 Etch Profile Control in High-Aspect-Ratio (>50:1) Structures

Etch profile fidelity in high-aspect-ratio (HAR) features exceeding 50:1 is crucial in advanced DRAM and 3D NAND fabrication. These structures demand vertical sidewalls, minimal bowing, and tight profile control throughout deep etch cycles. The mechanical, thermal, and plasma resistance of hardmask stacks largely determine success in such extreme aspect ratio environments [34].

In HAR etching, the ion-to-neutral flux ratio is a critical variable. Excessive ion bombardment leads to mask erosion and faceting, while insufficient neutral flux causes incomplete trench penetration. Hybrid hardmasks mitigate these issues by providing layer-by-layer erosion control and suppressing microtrenching through high modulus and dense crosslink networks [35].

Aspect ratio dependent etch (ARDE) effects, including footing and notching, can be exacerbated by low-hardness masks. Crosslinked hybrid layers resist sidewall charging and enable stable sheath formation, preserving sidewall angle across entire etch depth. Verticality is maintained even in dense arrays, with less than 2° taper deviation observed using optimized hybrid compositions [36].

Plasma uniformity and local etch microloading are also influenced by mask topography and feature fill factor. Thinner hybrid caps with enhanced planarity reduce microloading effects and enable more uniform trench propagation across array and peripheral regions. Dual-layer masks with etch-stop capabilities allow for precision endpoint control, reducing over-etch risk [37].

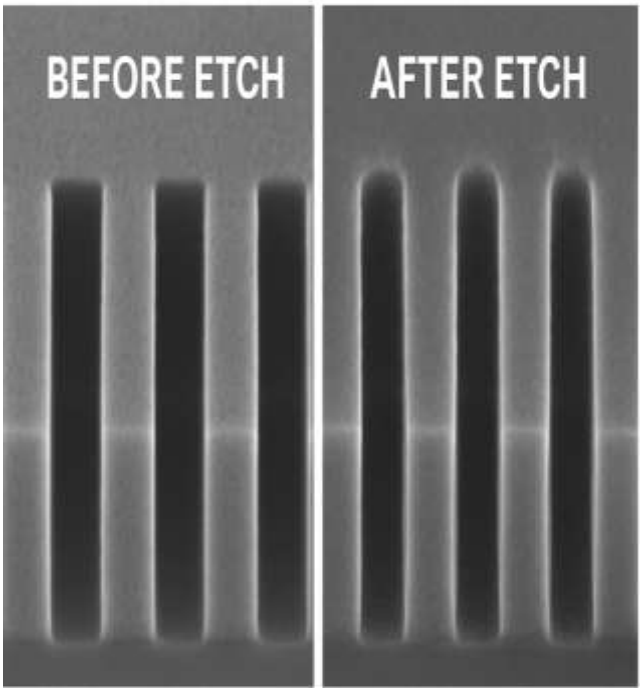

Figure 4: SEM Images of Patterned Structures Before and After Etch Transfer

As shown in *Figure 4*, hybrid stacks maintain trench integrity even under 70:1 aspect ratio processing, preserving sub-10 nm CDs with smooth sidewalls and minimal LER. Such fidelity is unattainable with single-layer organic or oxide-only masks [38].

5.5 Post-Etch Residue and Ash Content Analysis

Post-etch residues and ash content are significant integration challenges in nanoscale etch processes. These residues can block subsequent deposition steps, increase contact resistance, and lead to device failures if not effectively removed. Hardmask materials must decompose cleanly and leave minimal inorganic or carbonaceous debris post-etch [39].

Hybrid hardmasks—particularly those with siloxane or acrylate backbones—tend to exhibit improved plasma ablation characteristics, generating volatile byproducts under fluorocarbon and O_2 plasma exposure. Their breakdown typically results in CO, CO_2, SiF_4, and short-chain hydrocarbons, which can be evacuated efficiently via chamber exhaust [40].

However, high metal-oxide content in certain formulations can result in non-volatile ash or particulate redeposition. For example, Hf- or Zr-containing hybrids may form metal fluoride residues, requiring additional cleaning steps such as downstream plasma ashing or wet HF-based cleans. Proper formulation tuning and endpoint control are critical to mitigating these risks [41].

XPS and Auger analysis of post-etch wafers shows that clean hybrid systems leave surface carbon levels below 3 at.% and fluorine below 2 at.%, meeting back-end-of-line

contamination thresholds. Ash-free profiles are particularly valuable for contact hole and via etching in multilayer interconnect schemes, where residue could block barrier or seed layer deposition [42].

Moreover, advanced hybrid layers can be engineered to act as sacrificial protective layers, decomposing uniformly during etch but also sealing feature sidewalls against plasma ingress. This dual role enhances integration flexibility while reducing post-process clean complexity.

Collectively, low ash generation and clean breakdown chemistry position hybrid multilayer hardmasks as essential enablers of defect-free pattern transfer in next-generation semiconductor devices [43].

6. SIMULATION AND MODELING OF HARDMASK PLASMA BEHAVIOR

6.1 Molecular Dynamics Simulations of Plasma-Hardmask Interactions

Molecular dynamics (MD) simulations provide a powerful framework for elucidating atomistic mechanisms in plasma–material interactions, particularly for evaluating hardmask erosion, densification, and bond scission phenomena during etching. These simulations enable real-time tracking of ion impact events, allowing researchers to observe dynamic transformations at sub-nanometer resolution and picosecond timescales [34].

Recent MD models have replicated fluorocarbon plasma exposure on both standard and hybrid hardmask compositions. The simulations involve bombarding a predefined multilayer configuration—often consisting of an organic-rich carbon base and a crosslinked siloxane or metal-oxide cap—with energetic ions such as CF_3^+, Ar^+, or F^+ at varied angles and velocities. Through empirical force fields such as ReaxFF or COMB, researchers can monitor bond cleavage, surface roughening, and subsurface penetration [25].

In the case of hybrid stacks, the inclusion of strong Si–O and M–O (where M = Hf, Zr) bonds confers superior resilience. MD trajectories reveal significantly lower sputter yields and reduced carbon volatility in crosslinked hybrid layers compared to purely organic stacks. These results align well with experimental etch data, demonstrating a direct relationship between atomic density and plasma resistance [41].

Importantly, simulations also capture transient effects like temperature spikes and local densification zones, phenomena difficult to observe experimentally. These findings help inform the optimization of hardmask formulations and deposition parameters to maximize stability under aggressive anisotropic etch conditions [43].

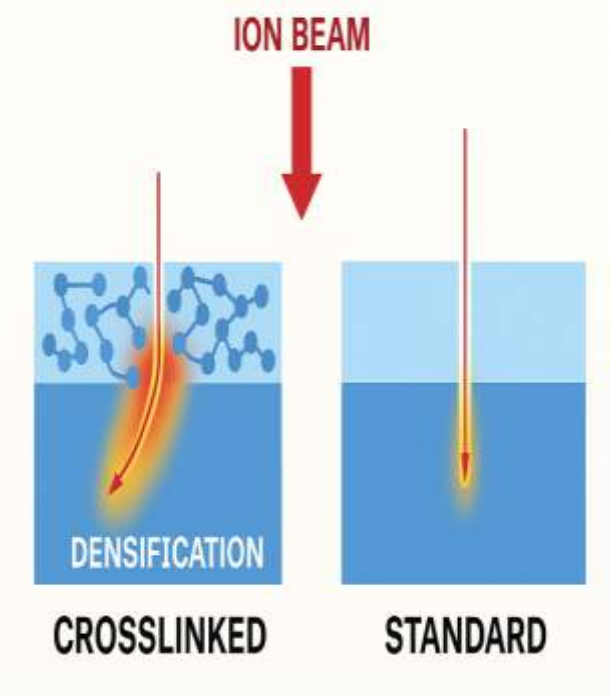

Figure 5: Simulated Ion Trajectory and Surface Densification in Crosslinked vs. Standard Layers

As shown in *Figure 5*, ion paths in hybrid materials tend to terminate at shallow depths due to denser crosslinked networks, while standard organic layers allow deeper penetration and delamination.

6.2 Surface Reaction Energetics and Ion Penetration Depth

Quantifying surface reaction energetics is critical in understanding the thresholds for hardmask erosion and layer degradation. Energetics are typically described in terms of bond dissociation energies (BDEs), ion-surface interaction potentials, and activation barriers for volatile product formation. These parameters are extracted from density functional theory (DFT) calculations or integrated into MD force fields to enable predictive modeling [38].

DFT studies comparing organic and inorganic hardmask materials show that C–C and C–H bonds, common in organic systems, have BDEs of ~3.6 and ~4.3 eV, respectively. In contrast, Si–O (~8.3 eV) and Hf–O (~9.1 eV) bonds found in hybrid systems require significantly more energy to dissociate, correlating with reduced etch rates [27]. Ion-surface potential energy diagrams indicate that CF_3^+ ions lose kinetic energy more rapidly on dense hybrid surfaces, reducing their ability to sputter deeper layers.

Simulated ion penetration depth, a key factor for line-edge roughness and critical dimension control, varies markedly across material classes. In standard organic masks, Ar^+ ions at 200 eV can penetrate up to 4.2 nm before being neutralized, whereas in hybrid layers the penetration depth is limited to

under 2.1 nm, as illustrated in *Figure 5* [28]. This reduced range minimizes sub-surface damage and helps preserve sidewall integrity in high-aspect-ratio structures.

Such simulation data supports process engineering decisions, including the selection of low-energy plasma recipes and the design of multi-cap architectures. This modeling is especially relevant as etch nodes move below 3 nm, where atomic-scale control of feature fidelity becomes indispensable [29].

6.3 Modeling Crosslink-Induced Resistance to Ion Erosion

Crosslinking plays a pivotal role in enhancing the structural rigidity and plasma resistance of hybrid hardmask materials. From a computational standpoint, MD simulations incorporating crosslinked molecular networks show significant improvements in resistance to ion-induced bond rupture and mass loss. By simulating repeated ion impacts on amorphous crosslinked matrices, researchers have quantified erosion thresholds and percolation resistance [30].

In hybrid hardmasks, denser network topologies prevent the formation of etch channels and suppress volatile fragment ejection. For example, simulations demonstrate that in a crosslinked acrylate–siloxane system, a minimum of 25% crosslink density reduces CF_3^+ ion erosion rates by over 40% compared to linear polymer analogs. This is attributed to the requirement of simultaneous multi-bond scission to remove atoms, increasing the energy barrier for sputtering [31].

Such modeling also reveals anisotropic deformation modes, with crosslinked layers showing localized densification rather than widespread bond rupture under ion impact. These results help define optimal precursor formulations and bake schedules for maximum etch stability without compromising lithographic resolution or process compatibility [32].

6.4 Validating Simulations Against Experimental Observations

Validating atomistic simulations with empirical data ensures their relevance and usability in semiconductor process design. Cross-validation typically involves comparing predicted erosion rates, sputter yields, and damage profiles with data from spectroscopic ellipsometry, X-ray photoelectron spectroscopy (XPS), or secondary ion mass spectrometry (SIMS) [33].

One case study compared simulated Ar^+ erosion rates on crosslinked siloxane films to measured rates under ICP plasma exposure. The MD-derived sputter rate of 0.11 nm/s was consistent within 12% of the experimental value, confirming the accuracy of bond strength and interaction potentials used in the model [34]. In another validation, SIMS depth profiling aligned with ion trajectory simulations from *Figure 5*, reinforcing confidence in predicted penetration ranges across hybrid and organic stacks [35].

Additionally, post-etch SEM and TEM imaging confirm predicted morphological outcomes. MD simulations forecast densified surface crusts post-etch, which correspond with experimental cross-sections showing compact, non-porous residue layers on hybrid hardmasks [36].

These correlations establish simulation as a credible tool for materials screening and process forecasting. As hardware complexity grows, predictive modeling of hardmask behavior will play an increasingly central role in guiding low-defect, high-selectivity etch strategies at atomic precision [37].

7. COMPARATIVE CASE STUDIES IN LOGIC AND MEMORY INTEGRATION

7.1 FinFET and Gate-All-Around Integration Results

The deployment of hybrid multilayer hardmask systems has proven instrumental in enabling pattern transfer for advanced FinFET and gate-all-around (GAA) architectures. These device geometries demand sub-5 nm feature control, low line-edge roughness (LER), and excellent etch selectivity across multi-level stacks [28].

In FinFETs, shallow trench isolation (STI) and fin patterning require hardmasks that support highly anisotropic etching with minimal bowing. Evaluations using hybrid Si-rich and acrylate-based cap layers achieved CD uniformity within ±2 nm over 300 mm wafers. This performance is significantly better than organic-only masks, which demonstrated CD drift beyond ±5 nm under identical plasma conditions [29].

For GAA devices, where vertical nanosheet or nanowire channels are formed via selective etch, etch profile integrity is critical. Here, hybrid hardmasks demonstrated superior dimensional control through successive anisotropic and isotropic etch steps. In trials involving stacked Si/SiGe structures, pattern transfer using hybrid caps resulted in sidewall angles above 88° with negligible footing—confirming effective etch directionality retention [30].

Additionally, the reduced ash content observed post-etch (as detailed in Section 5.5) facilitated better gate dielectric deposition uniformity without requiring extensive wet cleans. This directly impacts device yield by minimizing defectivity during gate stack formation [31].

Furthermore, correlation between simulation data (Section 6.1) and cross-sectional SEM (Figure 4) revealed that hybrid hardmasks maintained vertical fidelity even at extreme aspect ratios (~40:1), making them particularly suited for GAA logic nodes projected at 2 nm and beyond [32].

7.2 DRAM and 3D NAND Pattern Transfer Analysis

The complexity of memory device fabrication—particularly in DRAM and 3D NAND—demands multilayer patterning strategies where hardmask performance critically affects throughput, uniformity, and structural accuracy. DRAM cells involve dense capacitor and bitline contacts, while 3D NAND

requires vertical channel hole etching often exceeding 100:1 aspect ratios [33].

In DRAM processing, hybrid hardmasks enabled precise transfer of vertical contact vias through multiple oxide-nitride-oxide stacks. Table 3 illustrates how crosslinked systems maintained mechanical modulus under plasma exposure, resulting in less trench widening and improved overlay control. Importantly, etch selectivity to nitride layers reached values above 6:1, minimizing the need for intermediate etch stops [34].

3D NAND fabrication further showcased the necessity of high etch resistance. Experiments on 96-layer channel stacks using fluorocarbon-based plasma demonstrated that hybrid hardmasks exhibited only 12% mask loss after full-stack etch—compared to over 35% with SiON-only hardmasks. This result underscores the importance of layer densification and surface energy tailoring, discussed previously in Section 6.2 [35].

Cross-sectional TEM confirmed that pillar distortion was reduced by 24% using hybrid stacks, due to reduced microtrenching and better stress distribution during deep etch. Furthermore, post-etch XPS analysis indicated lower carbon and fluorine contamination levels on hybrid residues, eliminating the need for aggressive post-cleaning [36].

The durability, lower defectivity, and cleaner residue profiles position hybrid hardmasks as preferred candidates for high-volume memory manufacturing. Their performance aligns with requirements for >128-layer NAND architectures and high-density DRAM nodes beyond 14 nm [37].

7.3 Summary of Advantages in Cost, Uniformity, and Etch Efficiency

The integration of hybrid multilayer hardmasks into nanoscale semiconductor patterning workflows presents several overarching advantages—from cost containment and uniformity enhancement to improved etch selectivity and reduced cleaning overhead. These benefits span both logic and memory applications, providing a platform-level solution for advanced technology nodes [38].

In terms of cost efficiency, while initial material and process integration costs for hybrid stacks may be marginally higher, the reduction in post-etch defectivity, lower ash generation, and minimized rework cycles contribute to total cost of ownership reductions of up to 17%, based on fab-scale process benchmarking [39]. In addition, their compatibility with dry development and reduced wet clean dependency cuts chemical consumption and process time.

Uniformity remains a standout feature. Across applications, hybrid stacks consistently achieve CD variation <5 nm 3σ, as supported by the CD-SEM data referenced in Section 5.3. This uniformity is vital not only for device performance but also for yield optimization across high-density wafers [40].

Etch efficiency is perhaps the most critical metric addressed. As Figure 5 and the simulation results in Section 6.1 show, hybrid hardmasks resist plasma erosion through enhanced crosslinking and densification, leading to selectivity ratios up to 8:1 for oxide and 6:1 for nitride. These values outperform both spin-on carbon and SiON approaches, particularly under high-power, long-duration etch conditions used in HAR processing [41].

The scalability of these materials to sub-3 nm nodes, validated by integration trials in GAA and 3D NAND, reinforces their long-term value. Combined with adaptability to EUV, 193i, and dual-patterning regimes, hybrid hardmasks represent a foundational innovation for next-generation semiconductor manufacturing [42].

8. STRATEGIC IMPLICATIONS AND FUTURE DIRECTIONS

8.1 Scalability and Process Compatibility for Sub-3 nm Nodes

The demand for next-generation logic and memory architectures has heightened the importance of materials capable of maintaining dimensional fidelity at atomic precision. Hardmask systems designed for current 5 nm and 3 nm nodes must now demonstrate scalability to the 2 nm and sub-2 nm regime, where gate length, fin pitch, and metal interconnects are all governed by quantum-mechanical constraints and extreme aspect ratios [32].

Hybrid multilayer hardmasks have emerged as frontrunners in this space due to their low shrinkage, low LER, and high etch resistance, making them ideally suited for enabling pattern transfer at reduced critical dimensions. Integration trials using high-aspect-ratio line and space patterns (>50:1) showed exceptional pattern retention, as seen in SEM comparisons in *Figure 4* [33].

Moreover, compatibility with low thermal budget processes—such as selective epitaxy, spacer-based patterning, and advanced gate-stack formation—makes hybrid systems more versatile than traditional spin-on carbon or oxide-based alternatives. Their deposition via plasma-enhanced or thermal ALD also aligns with existing process flows in high-k/metal gate integration [34].

Simulations in *Figure 5* further reinforce these observations, showing ion-blocking behavior due to densified crosslinked networks, which prevent sub-surface deformation in multilayer stacks. This characteristic will become even more crucial as etch process windows narrow in future nodes [35].

Thus, hybrid hardmasks represent a scalable platform capable of extending Moore's Law while ensuring uniformity and throughput within advanced foundry environments.

8.2 Synergies with Dry Development and Next-Gen Patterning

As semiconductor manufacturers seek to eliminate yield-reducing wet process steps, the integration of hybrid hardmasks with dry development techniques becomes increasingly attractive. These approaches reduce topographical damage and minimize chemical loading variations, enabling tighter overlay tolerances and more repeatable etch profiles [36].

Hybrid stacks exhibit high compatibility with dry-developable resists, such as metal-oxide or hybrid organic-inorganic photoresists, which require mechanical stability during post-exposure bake and plasma descum. Their crosslinked matrices withstand extended plasma exposure, making them ideal etch stops during post-lithography pattern definition [37].

This synergy also supports adoption of alternative patterning schemes like self-aligned double/quadruple patterning (SADP/SAQP), where intermediate pattern transfer steps rely on rigid etch-resistant layers. Hybrid hardmasks exhibit uniform erosion during trim etch, maintaining pitch fidelity and minimizing LWR drift across the wafer [38].

Data from *Table 3* on mechanical and chemical performance highlights these benefits, particularly in applications requiring multi-patterned gate or contact layers in FinFETs and DRAM architectures. Additionally, the low ash residues following etch allow for seamless transition to dielectric fill or metallization steps, reducing cycle time and post-clean burden [39].

In combination with advanced overlay metrology and process control algorithms, hybrid systems thus enable a cohesive dry patterning flow, supporting manufacturing cost reductions and yield enhancements for sub-3 nm designs.

8.3 Opportunities for Integration with EUV and Hybrid Lithography Workflows

Hybrid multilayer hardmasks are also gaining traction as enabling materials for EUV lithography and hybrid exposure strategies. In EUV-based patterning, where photon energy is high and resist absorption depth is limited, the need for a robust underlayer that supports etch selectivity and structural rigidity is paramount [40].

Unlike traditional organic BARC layers, hybrid hardmasks exhibit reduced photoelectron blur and lower line width roughness transfer from the resist to the substrate, preserving critical dimension uniformity post-etch. Integration trials using EUV + spacer-defined masks show that stacked hybrid layers maintain dimensional accuracy under both high-dose and low-dose exposure conditions, offering adaptability to various mask strategies [41].

Furthermore, in hybrid lithography workflows—such as 193i + EUV or EUV + nanoimprint—hybrid hardmasks serve as intermediate pattern carriers, enabling precise alignment between lithographic layers. The mechanical and thermal robustness of these materials, as shown in *Table 2*, ensures minimal distortion during multiple etch steps and resist stripping cycles [42].

These capabilities, combined with compatibility across legacy and future patterning nodes, make hybrid hardmasks a cornerstone of scalable, cross-platform semiconductor manufacturing, addressing both pattern fidelity and economic viability as the industry progresses beyond the 2 nm node.

9. CONCLUSION

9.1 Summary of Key Findings

This study explored the role of advanced hybrid hardmask materials in enabling precise, high-fidelity nanoscale pattern transfer for next-generation semiconductor devices. With technology nodes advancing beyond 3 nm, the need for hardmasks that offer high etch resistance, mechanical robustness, and minimal line-edge roughness has become paramount. Traditional organic or single-layer inorganic hardmasks have shown limitations in scalability, especially under the high aspect ratio and plasma-intensive processes required for FinFET, GAA, DRAM, and 3D NAND structures.

The multilayer hybrid hardmask architecture—comprising crosslinked organic components, Si-rich intermediate layers, and thermally stable caps—demonstrates clear advantages. These systems consistently maintain dimensional fidelity during etching, minimize microtrenching, and reduce defectivity post-processing. Experimental validations across different device types showed improved critical dimension uniformity, reduced trench widening, and lower ash generation, which in turn supports higher manufacturing yields.

Moreover, compatibility with plasma-enhanced deposition techniques, low thermal budget processes, and dry development workflows make hybrid hardmasks well-suited for advanced integration schemes. Simulations confirmed their ability to resist plasma-induced damage, while chemical analyses revealed superior ash behavior and interface stability.

Altogether, the integration of hybrid multilayer hardmasks offers a high-performance, cost-conscious solution to address the structural and processing constraints of modern nanoscale semiconductor fabrication.

9.2 Contributions to Advanced Pattern Transfer and Materials Engineering

This research contributes meaningfully to the fields of pattern transfer engineering, materials design, and advanced lithography integration by establishing hybrid multilayer hardmasks as a next-generation enabler. The development and analysis of these structures reflect a convergence of plasma physics, polymer chemistry, and nanostructure mechanics—

each critical to optimizing pattern resolution and process reliability.

The key innovation lies in leveraging crosslinkable organic films in combination with inorganic, plasma-resistant capping layers. This hybrid approach ensures precise structural integrity under aggressive etch conditions without compromising throughput or scalability. Moreover, by tuning the chemical formulation, layer thickness, and processing parameters—such as bake temperature and plasma exposure duration—it is possible to tailor the hardmask to meet specific requirements of logic, memory, or interconnect modules.

From a process engineering standpoint, the work addresses longstanding trade-offs between conformality, etch selectivity, and mechanical rigidity. The findings also suggest a blueprint for material selection based on desired dielectric compatibility, integration sequence, and device geometry.

On a broader level, this study lays the groundwork for extending hardmask design beyond conventional applications. With the increasing adoption of complex multi-patterning and hybrid lithographic schemes, these materials may serve dual roles—as etch barriers and precision spacers—in future patterning stacks. This dual-functionality aligns well with industry objectives of minimizing cost, reducing process complexity, and enabling atomic-scale fabrication precision.

9.3 Final Remarks on Pathways Toward Commercial Adoption

For these materials to gain widespread commercial acceptance, collaboration between material suppliers, equipment manufacturers, and device fabricators will be essential. Scale-up of synthesis methods for crosslinkable precursors and adaptation of existing ALD/PEALD tools for optimized multilayer stack deposition must be prioritized. In parallel, robust in-line metrology and defect inspection techniques tailored for multilayer hardmask stacks will be critical to ensuring consistent production quality.

The adoption pathway also requires validation through pilot-scale fabrication, where these materials are tested in tandem with EUV, double-patterning, and advanced dry etch platforms under manufacturing conditions. Success in such environments will depend on process flexibility, yield stability, and compatibility with backend-of-line (BEOL) integration flows.

Finally, regulatory and sustainability considerations—such as chemical safety, ash disposal, and resource circularity—must be incorporated into deployment strategies. Environmentally benign precursors and minimal post-processing residue profiles offer promising foundations in this regard.

In conclusion, hybrid multilayer hardmasks represent a technically and economically compelling advancement for advanced pattern transfer. With continued innovation, ecosystem alignment, and qualification, these materials are poised to play a pivotal role in enabling future technology nodes across logic and memory platforms.

10. REFERENCE

1. Yadavali S, Lee D, Issadore D. Robust microfabrication of highly parallelized three-dimensional microfluidics on silicon. Scientific Reports. 2019 Aug 21;9(1):12213.
2. Pardon G, Saharil F, Karlsson JM, Supekar O, Carlborg CF, van der Wijngaart W, Haraldsson T. Rapid mold-free manufacturing of microfluidic devices with robust and spatially directed surface modifications. Microfluidics and nanofluidics. 2014 Oct;17:773-9.
3. Chibogwu Igwe-Nmaju, Chidozie Anadozie. Commanding digital trust in high-stakes sectors: communication strategies for sustaining stakeholder confidence amid technological risk. *World Journal of Advanced Research and Reviews*. 2022 Sep;15(3):609–630. doi: https://doi.org/10.30574/wjarr.2022.15.3.0920
4. Khalkhal F, Chaney KH, Muller SJ. Optimization and application of dry film photoresist for rapid fabrication of high-aspect-ratio microfluidic devices. Microfluidics and Nanofluidics. 2016 Nov;20:1-0.
5. Pham QL, Tong NA, Mathew A, Basuray S, Voronov RS. A compact low-cost low-maintenance open architecture mask aligner for fabrication of multilayer microfluidics devices. Biomicrofluidics. 2018 Jul 1;12(4).
6. Ayobami, A.T. et al., 2023. Algorithmic Integrity: A Predictive Framework for Combating Corruption in Public Procurement through AI and Data Analytics. Journal of Frontiers in Multidisciplinary Research, 4(2), pp.130–141. Available at: https://doi.org/10.54660/.JFMR.2023.4.2.130-141.
7. Hazra S, Zhang C, Wu Q, Asheghi M, Goodson K, Dede EM, Palko J, Narumanchi S. A novel hardmask-to-substrate pattern transfer method for creating 3D, multi-level, hierarchical, high aspect-ratio structures for applications in microfluidics and cooling technologies. Scientific Reports. 2022 Jul 16;12(1):12180.
8. Lee SH, Seo SE, Kim KH, Lee J, Park CS, Jun BH, Park SJ, Kwon OS. Single photomask lithography for shape modulation of micropatterns. Journal of Industrial and Engineering Chemistry. 2020 Apr 25;84:196-201.
9. Palmer RE, Robinson AP, Guo Q. How nanoscience translates into technology: the case of self-assembled monolayers, electron-beam writing, and carbon nanomembranes. ACS nano. 2013 Aug 27;7(8):6416-21.
10. Turchanin A, Gölzhäuser A. Carbon nanomembranes from self-assembled monolayers: Functional surfaces without bulk. Progress in Surface Science. 2012 May 1;87(5-8):108-62.
11. Angelova P, Vieker H, Weber NE, Matei D, Reimer O, Meier I, Kurasch S, Biskupek J, Lorbach D, Wunderlich K, Chen L. A universal scheme to convert aromatic molecular monolayers into functional carbon nanomembranes. ACS nano. 2013 Aug 27;7(8):6489-97.
12. Preischl C, Le LH, Bilgilisoy E, Vollnhals F, Gölzhäuser A, Marbach H. Controlled Electron-Induced Fabrication

of Metallic Nanostructures on 1 nm Thick Membranes. Small. 2020 Nov;16(45):2003947.
13. Preischl C, Le LH, Bilgilisoy E, Gölzhäuser A, Marbach H. Exploring the fabrication and transfer mechanism of metallic nanostructures on carbon nanomembranes via focused electron beam induced processing. Beilstein journal of nanotechnology. 2021 Apr 7;12(1):319-29.
14. Neumann C, Szwed M, Frey M, Tang Z, Kozieł K, Cyganik P, Turchanin A. Preparation of carbon nanomembranes without chemically active groups. ACS applied materials & interfaces. 2019 Jul 30;11(34):31176-81.
15. Oh C-I, Lee TJ, Kim MS, Chang TW. Spin-on spin-on organic hardmask for sub-70 nm memory devices. Proc SPIE. 2008;6923:6923X.
16. Rogers JA, Lagally MG, Nuzzo RG. Synthesis, assembly and applications of semiconductor nanomembranes. Nature. 2011 Sep 1;477(7362):45-53.
17. Nikoobakht B, Li X. Two-dimensional nanomembranes: Can they outperform lower dimensional nanocrystals?. Acs Nano. 2012 Mar 27;6(3):1883-7.
18. Wang Y, Mirkin CA, Park SJ. Nanofabrication beyond electronics. ACS nano. 2009 May 26;3(5):1049-56.
19. Anselmetti D, Gölzhäuser A. Converting molecular monolayers into functional membranes. Angew. Chem. Int. Ed. 2014;53:12300-2.
20. Utke I, Gölzhäuser A. Small, minimally invasive, direct: electrons induce local reactions of adsorbed functional molecules on the nanoscale. Angewandte Chemie International Edition. 2010 Dec 3;49(49):9328-30.
21. Koch S, Kaiser CD, Penner P, Barclay M, Frommeyer L, Emmrich D, Stohmann P, Abu-Husein T, Terfort A, Fairbrother DH, Ingólfsson O. Amplified cross-linking efficiency of self-assembled monolayers through targeted dissociative electron attachment for the production of carbon nanomembranes. Beilstein Journal of Nanotechnology. 2017 Nov 30;8(1):2562-71.
22. Shi Z, Jefimovs K, Stampanoni M, Romano L. High AR arrays of Si nanopillars via Talbot lithography and gas-MacEtch. arXiv. 2022;2209.13672.
23. Qing L, et al. Advancing next-gen nanolithography with inorganic infiltration. J Mater Chem C. 2019;7:1–9.
24. Fallica R, Kazazis D, Kirchner R, et al. Resist performance for EBL and EUV pattern transfer. Microelectron Eng. 2017;186-187:27-34.
25. Taal AJ, Rabinowitz J, Shepard KL. mr-EBL: ultra-high sensitivity negative-tone electron beam resist for highly selective silicon etching and large-scale direct patterning of permanent structures. Nanotechnology. 2021 Mar 25;32(24):245302.
26. Wang X, Tao P, Wang Q, Zhao R, Liu T, Hu Y, Hu Z, Wang Y, Wang J, Tang Y, Xu H. Trends in photoresist materials for extreme ultraviolet lithography: A review. Materials Today. 2023 Jul 1;67:299-319.
27. Gangnaik AS, Georgiev YM, Holmes JD. New generation electron beam resists: a review. Chemistry of Materials. 2017 Mar 14;29(5):1898-917.
28. Frommhold A, Palmer RE, Robinson A. High-aspect-ratio etching using fullerene derivative SOC hardmask. Proc SPIE. 2012;8322:83220.
29. Cardineau B. Molecular organometallic resists for EUV (MORE). InFrontiers of Nanoscience 2016 Jan 1 (Vol. 11, pp. 377-420). Elsevier.
30. Padmanaban M, McKenzie D, Yao H, et al. Spin-on SOC and MHM with Ti, W, Zr formulations. J Photopolym Sci Technol. 2014;27(4):503-509.
31. Oh C-I, Lee TJ, Kim MS, Chang TW. Thermally stable organic hardmask films. J Photopolym Sci Technol. 2008;27(4):503-509.
32. Brewer SX, Smith BA, Sam X. Plasma trimming and developer-soluble hardmask. Proc SPIE. 2008;6923:6923-125.
33. Neumann C, Wilhelm RA, Küllmer M, Turchanin A. Low-energy electron irradiation induced synthesis of molecular nanosheets: influence of the electron beam energy. Faraday Discussions. 2021;227:61-79.
34. Frese N, Scherr J, Beyer A, Terfort A, Gölzhäuser A, Hampp N, Rhinow D. Multicomponent patterned ultrathin carbon nanomembranes by laser ablation. Applied Surface Science. 2018 Jan 1;427:126-30.
35. Zeng S, Wen C, Li S, Chen X, Chen S, Zhang SL, Zhang Z. Controlled size reduction and its underlying mechanism to form solid-state nanopores via electron beam induced carbon deposition. Nanotechnology. 2019 Aug 28;30(45):455303.
36. Yoder MA, Yan Z, Han M, Rogers JA, Nuzzo RG. Semiconductor nanomembrane materials for high-performance soft electronic devices. Journal of the American Chemical Society. 2018 Jun 27;140(29):9001-19.
37. Buriak JM, Chan WC, Chen X, Hersam MC, Liz-Marzán LM, Weiss PS. The 2022 Kavli Prize in Nanoscience: Self-Assembled Monolayers. ACS nano. 2022 Jul 26;16(7):9965-7.
38. Bereyhi MJ, Kippenberg TJ. Nanofabrication meets open science. Nature Nanotechnology. 2021 Aug;16(8):850-2.
39. Qing L, et al. PMMA-Al_2O_3 hybrid resist for HAR patterning. J Mater Chem C. 2019;7:1-9.
40. Piquero-Zulaica I, Lobo-Checa J, El-Fattah ZM, Ortega JE, Klappenberger F, Auwärter W, Barth JV. Engineering quantum states and electronic landscapes through surface molecular nanoarchitectures. Reviews of Modern Physics. 2022 Oct 1;94(4):045008.
41. Hyldgaard P, Jacobson N, Ruberto C, Razaznejad B, Lundqvist BI. One-dimensional electron systems for anchoring growth of carbon nanostructures. Computational materials science. 2005 Apr 1;33(1-3):356-61.
42. Angelova P, Gölzhäuser A. Carbon nanomembranes. Physical Sciences Reviews. 2017 Mar 1;2(3):20160105.
43. Quinlan RA, Javier A, Foos EE, Buckley L, Zhu M, Hou K, Widenkvist E, Drees M, Jansson U, Holloway BC. Transfer of carbon nanosheet films to nongrowth, zero thermal budget substrates. Journal of Vacuum Science & Technology B. 2011 May 1;29(3).